Mechanics of Advanced Composite Structures 4 (2017) 169-177

Semnan University

Mechanics of Advanced Composite Structures

journal homepage: http://MACS.journals.semnan.ac.ir

Using the Taguchi Method for Experimental and Numerical Investigations on the Square-Cup Deep-Drawing Process for Aluminum/Steel Laminated Sheets

M. Mahmoodi *, H. Sohrabi

School of Mechanical Engineering, Semnan University, Semnan, Iran

PAPER INFO

Paper history:
Received 2017-04-15
Revised 2017-05-06
Accepted 2017-07-01

Keywords:
Deep drawing
Laminated sheet
Square
Taguchi
Finite element simulation

DOI: 10.22075/MACS.2017.11051.1108

ABSTRACT

The effects of input parameters on the square-cup deep-drawing process for a two-layer aluminum/steel laminated sheet were investigated. Each layer was 0.7 mm thick, and the input parameters covered in the investigation were punch nose radius (PR), die shoulder radius (DR), the clearance between a punch and die (CPD), blank holder force (BHF), and layer arrangement (LA). The effects of the input parameters on wrinkling and thinning defects were determined by finite element simulation and Taguchi's design of experiments. Experimental tests were conducted to validate the finite element analysis results. Results indicated that the parameter exerting the greatest effect on thinning defects was PR, followed by LA relative to the other parameters. BHF had the highest influence on the wrinkle height of the two-layer aluminum/steel sheet. Optimization was conducted, and the optimum input parameter values that caused the least wrinkling and thinning defects were 5.35 mm for DR, 8.35 mm for PR, 6000 N for BHF, and 1.3 t for CPD.

1. Introduction

Deep drawing is a process for the formation of sheet metals, in which a blank is drawn radially by the mechanical action of a punch into a die or forming cavity. This process involves several input parameters, including the die shoulder radius (DR), punch nose radius (PR), blank holder force (BHF), and the clearance between a punch and die (CPD).

Because of the combination of special characteristics in multilayer sheets, such as corrosion resistance and electrical resistance, these materials have been extensively used in modern industries, including automobile and aerospace manufacturing [1]. Investigating the behavior of multilayer and, more specifically, double-layer sheet metals is essential to the deep-drawing process. By means of stretching and deep-drawing processes, Harhash et al. [2] studied the mechanical properties and formation behaviors of laminated steel/polymer sandwich panels.

Wrinkling and tearing are two common defects encountered in the deep-drawing process. Preventing these defects necessitates the use of an appropriate BHF value. Previous research confirmed the key role of BHF in the creation or prevention of the aforementioned problems [3, 4]. Kitayama et al. [5] used a system of adjustable BHFs and closed-loop algorithms to achieve an optimal BHF in square-section deep drawing. Savas et al. [6] examined the effects of die and blank holder shapes on the quality of deep drawing. In their experimental investigations, the authors demonstrated that the angle between a die surface and blank affects the distribution of BHF and forming force. Asadian et al. [7] probed into the deep drawing of tailor-welded interstitial free steel blanks with non-uniform BHF.

Aside from BHF, PR and DR are two other effective parameters in sheet metal formation via deep drawing; the optimum values of these parameters figure importantly in the quality of produced parts. Behrens [8] analyzed the effects of different tool geometries on the limiting drawing ratio in micro deep drawing.

Many researchers have used the finite element method to obtain appropriate parameters [9–12].

* Corresponding author, Tel.: +98-23-33383345; Fax: +98-23-33654122

E-mail address: mahmoodi@semnan.ac.ir

Sezek et al. [13], for example, used finite element simulation and experimental tests to investigate the deep drawing of blank sheets with circular sections. Their objective was to explore effective parameters and thereby improve the drawing ratio of workpieces and reduce BHF. Watiti et al. [14] applied experimental and finite element analyses to develop a methodology for determining the forming limits of AZ31 magnesium alloy and optimal forming parameters, such as PR, temperature, profile radius, and forming depth. Ghaffari et al. [15] developed a finite element model as a coupled thermomechanical model for the deep drawing of AZ31 alloy sheet. Castillo et al. [16] applied theoretical, numerical, and experimental techniques to obtain the allowable height for the deep drawing of single-layer steel sheets with square sections. Hashemi et al. [17] studied the probability of failure in hydrodynamic deep drawing. Neto et al. [18] conducted a finite element analysis of the reverse deep drawing of a cylindrical cup, for which the authors modeled forming tools as either rigid or deformable bodies to evaluate the elastic deformation of the tools.

Padmanabhan et al. [19] used the Taguchi technique to explore the effects of DR, BHF, and friction coefficient on the thickness variations of single-layer blanks. Using the same technique, Reddy et al. [20] studied the influence of DR, BHF, and a parameter disregarded by Padmanabhan et al., namely, PR [19].

Of the few studies directed toward multilayer sheet metal forming, that of Morovvati et al. [1] involved the use of numerical and experimental techniques to investigate the wrinkling and tearing defects that occur in double-layer metal sheets during the deep drawing of circular sections. Atrian and Fereshteh-Sanaiee [21] carried out finite element analysis and experimental tests to study the deep drawing of double-layer aluminum/brass sheets with circular sections. The authors determined the location of tearing that occurred in the experiments.

The purpose of the present work was to investigate the wrinkling and tearing defects that occur in a double-layer metal sheet during square-section deep drawing. This research also examined the effects of PR, DR, BHF, CPD, and layer arrangement (LA) on the aforementioned defects. To these ends, Taguchi's design of experiments was used and a finite element simulation was carried out. The simulation results were then validated by experimental tests.

2. Materials and methods

A double-layer blank sheet made of St14 steel and 1200 aluminum was used in the experiments. Each layer of the material was 0.7 mm thick, and the initial blank was square with a dimension of 80 mm. The aluminum/steel laminated sheet was produced by explosive forming [22, 23]. The mechanical properties of the layers are listed in Table 1.

A schematic of the die fabricated for the experiments is shown in Figure 1, and the experimental die setup is depicted in Figure 2. This assembly includes the die, punch, blank holder, and guide bars. The die is made of CK45 steel. Its surface was hardened through carburization at 900°C for 9 hours, after which it was polished to prevent wear and corrosion.

The coefficients of friction between different contact surfaces are presented in Table 2. The blank holder system of the die was designed in such a way that a variable BHF of 2000 to 10000 N can be achieved. The tests were performed using a 200-ton hydraulic press with a speed of 0.17 mm/s.

ABAQUS software and explicit analysis were adopted to simulate the deep-drawing process for the selected material. Figure 3 illustrates the geometrical model of the die used in the square-section deep-drawing process. Given geometrical symmetry, only one-quarter of the entire model was analyzed.

In the simulation, fixed boundary conditions (zero displacement) were applied to the die. The blank holder and punch were assigned one degree of freedom in the vertical direction (punch axis). The two-layer sheet was modeled in the shell plane using four-node shell elements (S4R), and the "tie" constraint was defined. The die, punch, and blank holder were modeled using rigid surface elements (R3D4). The size of the elements used to model the sheets was 1 mm. As indicated in Figure 4, mesh size was obtained by using a mesh sensitivity diagram in accordance with changes in sheet thickness at a specific point for different element sizes.

Table 1. Mechanical properties of steel and aluminum sheets

	1200 Al	St14
Yield stress (MPa)	80.57	180.33
Young's modulus (GPa)	75	210
Poisson's ratio	0.33	0.3
Density (Kg/m^3)	2710	7800

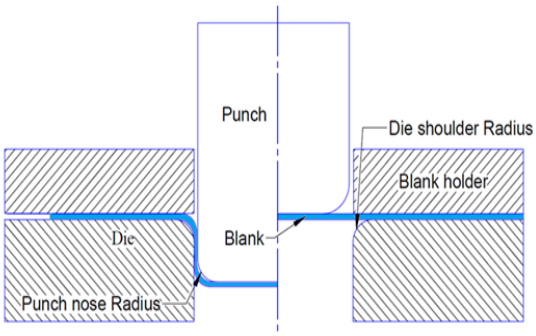

Figure 1. Schematic of the square-section deep-drawing process

Table 2. Coefficients of friction between contact surfaces [1]

Surface of contacts		Friction coefficient
Punch surface	Blank surface	0.12
Blank holder surface	Blank surface	0.1
Die surface	Blank surface	0.1

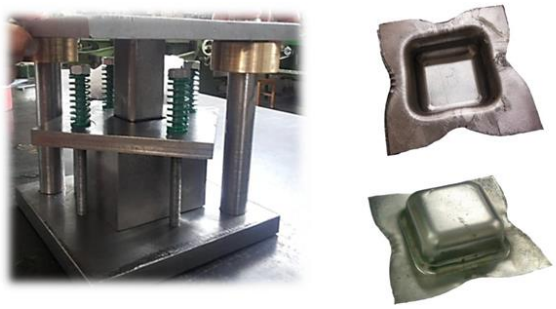

Figure 2. Experimental die setup and deformed part

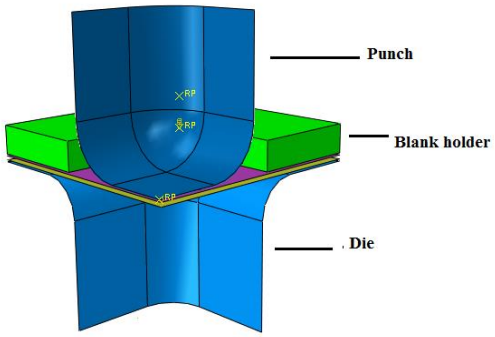

Figure 3. Geometrical model of the die

When difficulty is encountered in expressing the relationship between the input and output parameters of a process as a clear mathematical model, optimization techniques and design of experiments must be used to address the difficulty. Design of experiments is a scientific approach in which targeted changes in input factors affect a process or product. The resultant changes in the output are then examined, and extensive information is gained about the process or product.

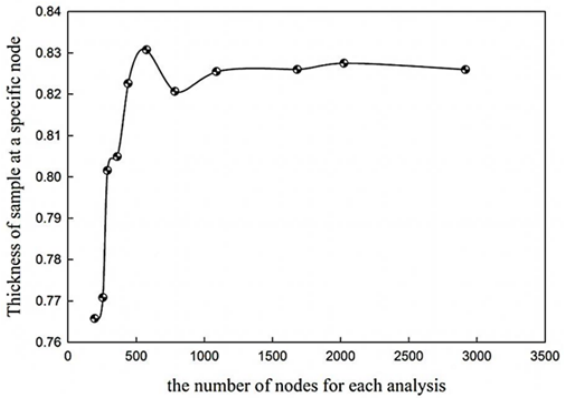

Figure 4. Mesh sensitivity diagram of the output values of thickness

This research employed Taguchi's design of experiments to explore the effects of several input parameters on the quality of double-layer samples produced via square-section deep drawing. Signal-to-noise (S/N) ratio analysis was then carried out, and the variations in output functions with respect to the input parameters were determined. ANOVA was then performed to identify the percentage of contribution of each parameter [24].

As previously stated, the input parameters considered in this work were PR, DR, BHF, CPD, and LA. Different values for these parameters are listed in Table 3. On the basis of preliminary tests conducted in a laboratory, the appropriate parameters and corresponding input values were chosen.

The number of tests proposed in the Taguchi method for examining the effects of input parameters on the quality of final samples produced by deep drawing is 16. These tests are listed in Table 4. Wrinkling and thinning defects were selected as the outputs of the Taguchi experiments for each sample. The maximum wrinkling wave height was regarded as the wrinkling defect index. In investigating thinning defects, the maximum thickness reduction in each layer was chosen as the thinning defect index. In the Taguchi analysis, the maximum thickness reduction in each layer served as the index for obtaining the optimal values of input parameters that minimize thinning. In other words, two outputs were used in each test with regard to thinning. The first output was the extent of thinning in the aluminum layer, and the second was the extent of thinning in the steel layer.

3. Results and discussion

As indicated in the results of the experiments and finite element analysis, specimen thickness increased or decreased at different regions. To investigate thinning in the deformed pieces, the maximum thickness reduction produced in each sample was chosen as the critical thinning index and regarded as the basis of the analysis. Figure 5 illustrates the results of Test #1 for the experiments indicated in Table 4. The initial thickness of the steel layer was 0.7 mm. Contours were plotted on the basis of the thickness values obtained following the deformation of the sample. As shown in Figure 5, after the sheet's deformation, its thickness underwent variations, which included an increase in thickness in some areas (e.g., wrinkle waves) and a reduction in thickness in other regions.

The maximum thickness increase and decrease in the steel layer were 13% and 16.7%, respectively. These values were obtained from equation 1.

$$Thinning\ percentage = \frac{Initial\ thickness - Final\ thickness}{Initial\ thickness} \times 100 \quad (1)$$

Table 3. Input parameters for the process and levels allocated to them (t = initial thickness)

Level	DR	PR	BHF (N)	CPD (mm)×t	LA
1	3.35	5.35	2000	1.1t	Al-St
2	4.35	6.35	4000	1.2t	St-Al
3	5.35	7.35	6000	1.3t	-
4	6.35	8.35	8000	1.4t	-

Table 4. L16 vertical arrays of the Taguchi method

Test number	Parameters				
	DR	PR	BHF	CPD	LA
1	1	1	1	1	1
2	1	2	2	2	1
3	1	3	3	3	2
4	1	4	4	4	2
5	2	1	2	3	2
6	2	2	1	4	2
7	2	3	4	1	1
8	2	4	3	2	1
9	3	1	3	4	1
10	3	2	4	3	1
11	3	3	1	2	2
12	3	4	2	1	2
13	4	1	4	2	2
14	4	2	3	1	2
15	4	3	2	4	1
16	4	4	1	3	1

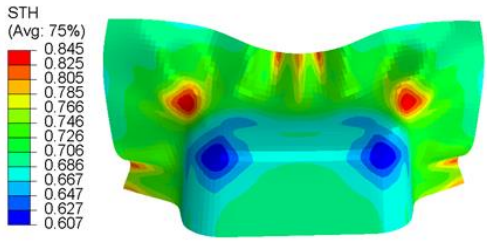

Figure 5. Contour of thickness variations in the steel layer of the aluminum/steel double-layer sheet (STH: thickness)

The maximum wrinkling wave height obtained from the simulation for the first test was 5.91 mm. To validate the simulation results, the wrinkle height of the sample obtained from the simulation was compared with that of the sample obtained from the experimental test (experimental wrinkle height = 6.1 mm). Figure 6 indicates good agreement between the finite element analysis and experimental results.

For the Taguchi analysis, the maximum percentage of thickness reduction was considered the criterion of thinning in the examined sample. The values of thinning for each test were recorded, and the results are presented in Figure 7. The graphs in the figure indicate the S/N ratios related to the values of each parameter. The S/N ratio was a statistical index obtained from equations 2 and 3.

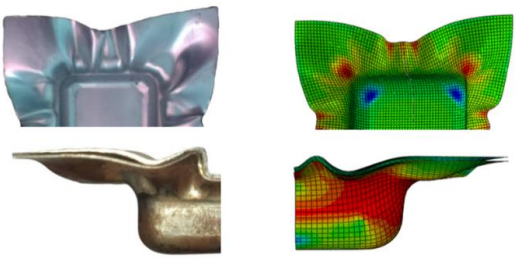

Figure 6. Comparison of the extent of wrinkling in the samples obtained from the simulation and experiments (Test #1, Table 3)

A high ratio indicates good quality of a final product with respect to a specified quality index. The abscissa of each diagram in Figure 7 shows the value of each parameter, and the ordinate of a diagram represents the S/N ratio at a given parameter value.

$$S/N = -10\times\log(MSD) \quad (2)$$

$$MSD=\frac{1}{n}\sum_{i=1}^{n}\frac{1}{(y_i)^2} \quad \text{(Larger is better.)} \quad (3)$$

$$MSD=\frac{1}{n}\sum_{i=1}^{n}(y_i)^2 \quad \text{(Smaller is better.)} \quad (4)$$

In equations 2–4, MSD denotes the mean square deviation, n represents the test number, and y is the smallest thickness measured in each test. The selection of the constraints "larger is better" and "smaller is better" depended on output index. In the analysis of thinning defects, the "larger is better" logic was adopted because the closer the maximum extent of thinning to the initial thickness of the sheet, the higher the quality of the produced sample. Figure 7 shows the diagrams pertaining to the effects of the input parameters on thickness deviation. As is indicated in the S/N ratio graph related to various values of the DR parameter, the optimum DR that minimizes the percentage of thinning in the double-layer sample was 5.35 mm. The S/N ratio at different values of the PR parameter was highest at the 4th-level radius (i.e., 8.35 mm). The S/N ratio diagram for PR demonstrates that with increasing PR, the occurrence of thinning and, thus, tearing in the sheets became less likely; choosing an appropriate PR enabled a greater drawing depth for the blank.

As shown in Figure 7, a BHF of 2000 N for the double-layer sheet led to the highest S/N ratio. This optimal BHF was the lowest among the four values allocated to this parameter.

The effects of BHF were compared with the results of Kitayama et al. [5] for the square-section deep drawing of single-layer sheets. The comparison indicated that with the application of a small BHF in the forming of single- and double-layer sheets, small thickness variations will occur in a deformed specimen. In previous works on the deep-drawing process [21, 25], different values were considered for CPD.

A necessary requirement in the current work, therefore, was to explore the optimal value of CPD. The S/N ratio diagrams for the effects of CPD on the maximum thickness deviation of the aluminum/steel sheet indicate that a CPD of 1.1 t was the optimal value for the prevention of sheet thinning.

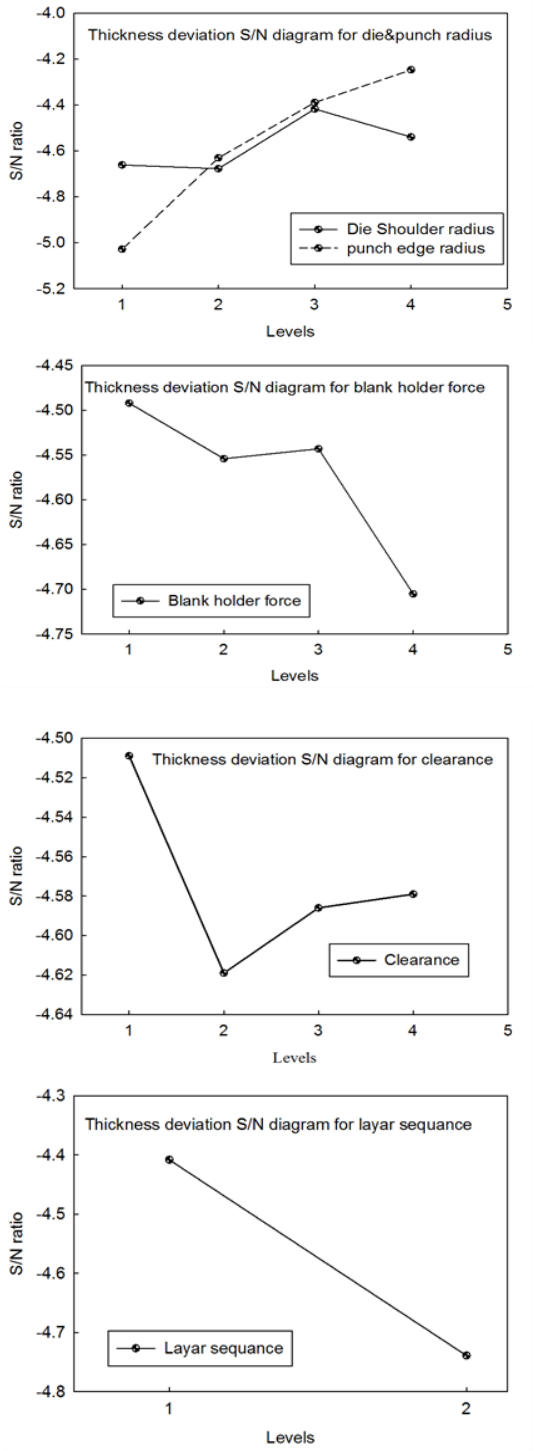

Figure 7. S/N ratio diagrams of the input parameters for thickness deviation

Investigation was also directed toward the effects of LA on maximum thinning. The Taguchi analysis results indicated that if the steel layer is in contact with the die surface and the aluminum layer is in contact with the blank holder, the deformed piece will undergo less thinning than when the order of sheets is reversed.

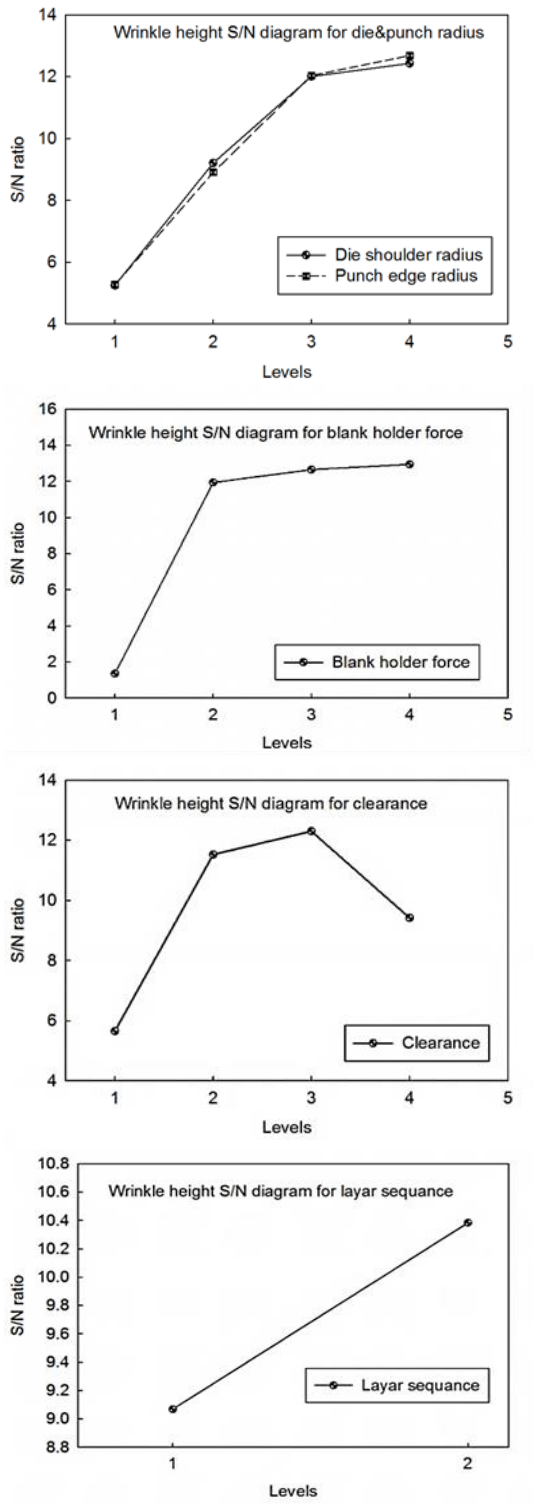

Figure 8. S/N ratio diagrams of the input parameters for wrinkle height

After the PR parameter, LA exerted the highest influence on thinning. This analysis demonstrated that LA is an effective parameter for the deep-drawing process.

To study the effects of the input parameters on wrinkling defects, the maximum wrinkling wave height was considered the index of such defect. The displacement of the blank holder along the punch axis was equal to the maximum wrinkle height and was used in the Taguchi analysis to evaluate the optimal values of the input parameters and obtain S/N ratio graphs. Figure 8 presents the diagrams pertaining to the effects of the input parameters on wrinkle height.

Table 5 lists the S/N ratios related to each parameter. For each parameter, two S/N ratios were allocated to every value of the parameter. The first S/N ratio of each parameter was based on the thinning index, and the second was based on the maximum wrinkle height of the double-layer sheet.

Table 5. ANOVA data table

Parameter	Level value	Expt no	Thickness (AL-ST)	Wrinkle height	S/Nij (Thinning)	S/Nij (Wrinkle height)
DR Level 1	3.35	1	0.5466-0.6073	5.9100	-4.661	5.252
		2	0.5694-0.6151	0.2840		
		3	0.5532-0.6236	0.2390	-4.677	9.213
		4	0.5578-0.6244	0.2220		
Level 2	4.35	5	0.5020-0.6032	1.1110	-4.417	12.009
		6	0.5352-0.6175	0.2660		
		7	0.5857-0.6233	0.2200	-4.539	12.432
		8	0.6038-0.6288	0.2210		
Level 3	5.35	9	0.5623-0.6083	0.2330		
		10	0.6083-0.6277	0.2189		
		11	0.5805-0.6179	0.3271		
		12	0.6179-0.6376	0.2376		
Level4	6.35	13	0.5861-0.6308	0.2408		
		14	0.6308-0.6393	0.2393		
		15	0.6009-0.6275	0.2275		
		16	0.6334-0.6489	0.2489		
			0.4905-0.6060			
			0.5549-0.6237			
			0.6083-0.6277			
			0.6323-0.6340			
PR Level 1	5.35	1	0.5466-0.6073	5.9100	-5.028	5.273
		5	0.5020-0.6032	0.2660		
		9	0.5623-0.6083	0.2330		
		13	0.4905-0.6060	0.2408		
Level 2	6.35	2	0.5694-0.6151	0.2840	-4.630	8.909
		6	0.5352-0.6175	1.1110		
		10	0.5805-0.6179	0.2189		
		14	0.6038-0.6288	0.2390		
Level 3	7.35	3	0.5532-0.6236	0.2393	-4.389	12.038
		7	0.5578-0.6244	0.2200		
		11	0.5857-0.6233	0.3271		
		15	0.6083-0.6277	0.2275		
Level 4	8.35	4	0.5623-0.6083	0.2220	-4.247	12.687
		8	0.6038-0.6288	0.2210		
		12	0.5861-0.6308	0.2376		
		16	0.6009-0.6334	0.2489		
			0.5532-0.6236			
			0.5857-0.6233			
			0.5861-0.6308			
			0.6083-0.6277			
			0.5578-0.6244			
			0.6038-0.6288			
			0.6009-0.6334			
			0.6323-0.6340			
BHF Level 1	2000	1	0.5466-0.6073	5.9100	-4.492	1.36
		6	0.5352-0.6175	1.1110		
		11	0.5861-0.6308	0.3271	-4.554	11.945
		16	0.6323-0.6340	0.2489		
Level 2	4000	2	0.5694-0.6151	0.2840	-4.543	12.655
		5	0.6009-0.6334	0.2660		
		12	0.6083-0.6277	0.2376		
		15	0.5578-0.6244	0.2275		
Level 3	6000	3	0.5532-0.6236	0.2390	-4.705	12.947
		8	0.6038-0.6288	0.2210		
		9	0.5623-0.6083	0.2330		
		14	0.6288-0.6393	0.2393		
Level 4	8000	4	0.5623-0.6083	0.2220		
		7	0.6083-0.6277	0.2200		
		10	0.5549-0.6237	0.2189		
		13	0.6237-0.6408	0.2408		
			0.5578-0.6244			
			0.5857-0.6233			
			0.5805-0.6179			
			0.4905-0.6060			
			0.5466-0.6073		-4.509	5.656
			0.5857-0.6233			
			0.6009-0.6334		-4.619	11.530
			0.5549-0.6237			
CPD Level 1	1.1t	1	0.5694-0.6151	5.9100	-4.586	12.302
		7	0.6038-0.6288	0.2200		
		12	0.5861-0.6308	0.2376		
		14	0.6009-0.6275	0.2393		
Level 2	1.2t	2	0.4905-0.6060	0.2840	-4.579	9.418
		8	0.5532-0.6236	0.2210		
		11	0.5578-0.6244	0.3271		
		13	0.5352-0.6175	0.2408		
Level 3	1.3t	3	0.5623-0.6083	0.2390		
		5	0.6083-0.6277	0.2660		
		10	0.5805-0.6179	0.2189		
		16	0.6323-0.6340	0.2489		
Level 4	1.4t	4	0.5466-0.6073	0.2220		
		6	0.5694-0.6151	1.1110		
		9	0.6151-0.6323	0.2330		
		15	0.5857-0.6340	0.2275		
LA Level 1	Al up-St down	1	0.5466-0.6073	5.9100	-4.408	9.069
		2	0.5694-0.6151	0.2840		
		7	0.6038-0.6288	0.2200		
		8	0.5623-0.6083	0.2210		
		9	0.6083-0.6277	0.2330		
		10	0.5532-0.6236	0.2189		
		15	0.5578-0.6244	0.2275		
		16	0.5352-0.6175	0.2489		
Level 2	Al down-ST up	3	0.5623-0.6083	0.2390	-4.739	10.384
		4	0.6083-0.6277	0.2220		
		5	0.5805-0.6179	0.2660		
		6	0.6179-0.6376	1.1110		
		11	0.5857-0.6233	0.3271		

12	0.6083-0.6340	0.2376
13	0.6277	0.2408
14	0.6323-0.6340	0.2393
	0.5532-0.6236	
	0.5578-0.6244	
	0.5020-0.6032	
	0.5352-0.6175	
	0.5861-0.6308	
	0.6009-0.6334	
	0.4905-0.6060	
	0.5549-0.6237	

By using the information in Table 5 and equations 5–8, the contribution of each parameter to thinning and wrinkling defects are obtained as follows:

$$\overline{S/N} = \frac{1}{16}\sum_{i=1}^{16}(S/N)_i \quad (5)$$

$$SS = \sum_{i=1}^{16}((S/N)_{ij} - \overline{S/N})^2 \quad (6)$$

$$SS_i = \sum_{i=1}^{4}((S/N)_{ij} - \overline{S/N})^2 \quad (7)$$

$$\%contribution = \frac{SS_i}{SS} \times 100 \quad (8)$$

The overall mean S/N ratio and the sum of squares due to variations around the overall mean are expressed as equations 5 and 6. For the i_{th} process parameter, the sum of squares due to variations about the mean is expressed as equation 7. This summation is over the two levels of study for LA and four levels of study for the other process parameters.

The contributions of the input parameters to the thickness deviation of the sheet are listed in Table 6.

According to the results, PR exerted the strongest effect on thinning in the aluminum/steel double-layer sheet. In investigating the effects of input parameters on the thickness deviation of single-layer stainless steel sheets during the deep-drawing of circular blanks and without consideration for PR as an input parameter, Padmanabhan et al. [19] determined the contribution of DR to thinning defects as close to 90%. This percentage leaves a very small proportion of contribution for other parameters, such as friction and BHF.

Table 6. Contributions of input parameters to thinning

Parameters	SSi	Contribution
DR	0.044	9.2%
PR	0.350	72.9%
BHF	0.025	5.2%
CPD	0.006	1.3%
LA	0.054	11.4%

Table 7. Contributions of input parameters to wrinkling

Parameters	SSi	Contribution
DR	32.55	17.3%
PR	34.60	18.4%
BHF	93.86	49.8%
CPD	26.55	14.0%
LA	0.86	0.5%

The contributions of the input parameters to the maximum wrinkle height were obtained. The results are presented in Table 7, which shows that BHF was the most effective parameter, as evidenced by its contribution of 49.8%. The optimum values of the input parameters differed depending on the selected quality indices (maximum thickness reduction and maximum wrinkling wave height). With regard to the wrinkle height index, for instance, the optimum value of BHF was 8000 N, but with respect to the thinning index, this value was 2000 N.

To select an appropriate BHF value in a way that minimizes both wrinkling and thinning defects, the contribution of this parameter to the defects should be evaluated. BHF contributed 5.2% and 49.8% to thickness variations and wrinkling defects, respectively. Given that this parameter had a much stronger effect on wrinkling defects than thinning defects, the magnitude of this force must be close to its optimal value on the basis of the wrinkle height index. Thus, the 3rd-level value of the BHF parameter (i.e., 6000 N) was the most suitable for the formation of the aluminum/steel double-layer sheet.

Because DR contributed 17.3% to wrinkling and 9.2% to thinning, its 3rd-level value (i.e., 5.35 mm) was considered the optimum value of the parameter. From the perspective of both indices, the 4th-level value of PR (i.e., 8.35 mm) was the optimal value for this parameter. CPD affected wrinkling to an extent of 14% and thinning to a degree of 1.3%. Given that its contribution to wrinkling is much greater than its contribution to thinning, the 3rd-level value of CPD (i.e., 1.3 t) was the optimum value of this parameter.

LA affected thinning and wrinkle height to an extent of 11.4% and 0.5%, respectively, indicating the significance of this parameter in the thinning and eventual tearing of the double-layer sheet used in the square-section deep drawing. In view of this significance, the 1st-level arrangement of this parameter (i.e., Steel is in contact with the die surface.) was considered the optimal arrangement for this input parameter.

The optimum values of the input parameters are given in Table 8.

Table 8. Optimum values of input parameters in the square-section deep drawing of aluminum/steel double-layer sheet

Parameters	
DR	5.35 mm
PR	8.35 mm
BHF	6000 N
CPD	1.3 t (level 3)
LA	Al up-St14 down (level 1)

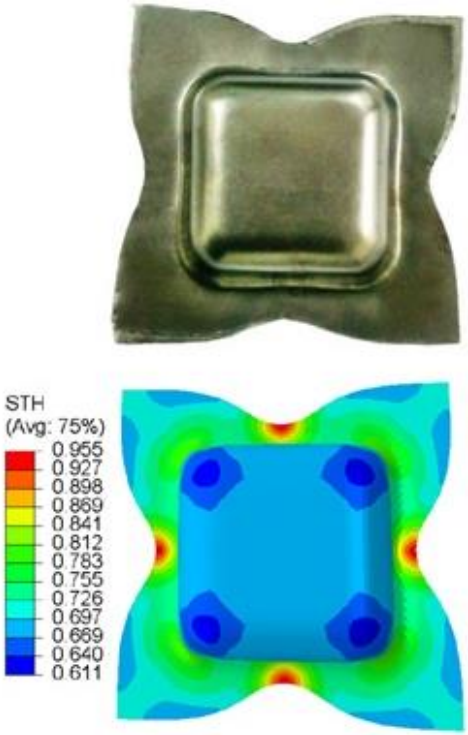

Figure 9. Comparison of the samples obtained from the experimental tests and finite element simulation based on the optimum values of the input parameters (STH: thickness)

The experimental and simulated samples obtained from this process through the optimum values of input parameters are presented in Figure 9. The figure indicates that the samples obtained from the experimental tests and the finite element simulation showed good agreement.

4. Conclusion

The square-section deep-drawing process for blanks is highly sensitive to the values of input parameters. Preventing thinning necessitates the appropriate selection of optimal PR and LA in double-layer sheets. To prevent wrinkling, an essential requirement is to choose an optimal BHF. As indicated in the results, BHF must also have an intermediate value between the optimum values associated with wrinkling and thinning indices because although a large BHF prevents wrinkling, it contributes to tearing. Additionally, even though a small BHF reduces the extent of thinning in sheets, it causes wrinkling.

The design of experiments based on the Taguchi method of vertical arrays can be used to determine the effects of parameters in the deep-drawing process. The optimum values obtained through this method for the input parameters of the deep drawing of an aluminum/steel double-layer sheet were 5.35 mm for DR, 8.35 mm for PR, 6000 N for BHF, and 1.3 t for CPD. LA was associated with the level 1 arrangement (i.e., The aluminum layer is in contact with the blank holder, and the steel layer is in contact with the die surface.).

The ANOVA of the input parameters indicated that BHF (with a contribution of 49.8%) exerted the strongest influence on the occurrence of wrinkling and that PR (with a contribution of 72.9%) posed the greatest effect on the occurrence of thinning. These parameters were therefore the most significant among the examined input parameters.

References

[1] Morovvati MZ, Fatemi A, Sadighi M. Experimental and finite element investigation on wrinkling of circular single layer and two-layer sheet metal in deep drawing process. *Int J Adv Manuf Technol* 2011; 54:113-121.

[2] Harhash M, Carradò A, Palkowski H. Mechanical properties and forming behaviour of laminated steel/polymer sandwich systems with local inlays – Part 2: Stretching and deep drawing. *Compos Struct* 2017; 160: 1084–1094.

[3] Hauptmann M, Weyhe J, Majschak J. Optimisation of deep drawn paperboard structures by adaptation of the blank holder force trajectory. *J Mater Proc Technol* 2016; 232: 142–152.

[4] Wang Y, Huang G, Liu D, et al. Influence of blank holder type on drawability of 5182-O aluminum sheet at room temperature. *Trans Nonferrous Metals* 2016; 26: 1251–1258.

[5] Kitayama S, Hamano S, Yamazaki K, Kubo T, Nishikawa H, Kinoshita H. A closed-loop type algorithm for determination of variable blank holder force trajectory and its application to square cup deep drawing. *The International J Adv Manuf Technol* 2010; 51:507-517.

[6] Savas V, Secgin O. An experimental investigation of forming load and side-wall thickness obtained by a new deep drawing die. *Int J Mater Forming* 2010; 3(3):209-213.

[7] Asadian MH, Morovvati MR, Mirnia MJ, Dariani BM. Theoretical and experimental investigation of deep drawing of tailor-welded IF steel blanks with non-uniform blank holder forces. *Proc IMechE Part B J Eng Manuf* 2015; 1-15

[8] Behrens G, Trier FO, Tetzel H, Vollertsen F. Influence of tool geometry variations on the limiting draw-ing ratio in micro deep drawing. *The Int J Mater Forming* 2016; 9: 253-258.

[9] Ouyang Y, Lee MS, Moon J, Kang CG. The effect of the blank holding force on formability in hot

deep drawing of boron steel considering heat transfer phenomena and friction coefficient by simulation and experimental investigation. *Proc IMechE B J Eng Manuf* 2012; 226: 1506-1518.

[10] Ren LM, Zhang SH, Palumbo G, Tricarico L. Warm deep drawing of magnesium alloy sheets-formabil-ity and process conditions. *Proc IMechE Part B J Eng Manuf* 2008; 222: 1347-1354.

[11] Moradi M, Golchin E. Investigation on the effects of process parameters on laser percussion drilling using finite element methodology; statistical modelling and optimization. *Latin Am J Solids Struct* 2017; 14(3): 464-484.

[12] Moradi M, Ghoreishi M, Rahmani A. Numerical and Experimental Study of Geometrical Dimensions on Laser-TIG Hybrid Welding of Stainless Steel 1.4418, *J Modern Proc Manuf Production* 2016; 5(2): 21-31.

[13] Sezek S, Savas V, Aksakal B. Effect of die radius on blank holder force and drawing ratio: A model and experimental investigation, *Mater Manuf Proc* 2010; 25:557-564.

[14] Watiti VB, Labeas GN. Finite Element Optimization of Deep Drawing Process Forming Parameters for Magnesium Alloys. *Int J Mater Forming* 2010; 3:97-100.

[15] Ghaffari TD, Worswick MJ, Mckinley J, Bagheriasl R. AZ31 magnesium deep drawing experiments and finite element simulation. *Int J Mater Forming* 2010; 3: 159-162.

[16] Medellin-Castillo HI, Garcia-Zugasti PJ. et al. Analysis of the allowable deep drawing height of rectangu-lar steel parts. *Int J Adv Manuf Tech* 2013; 66:371-380.

[17] Hashemi A, Hoseinpour Gollo M, Seyedkashi S. Study of Al/St Laminated Sheet and Constituent Layers in Radial Pressure Assisted Hydrodynamic Deep Drawing. *Mater Manuf Proc* 2017; 32(1):54-61.

[18] Neto DM, Coër J, Oliveira MC , Alves JL, Manach PY, Menezes LF. Numerical analysis on the elastic deformation of the tools in sheet metal forming processes. *Int J Solids Struct* 2016; 100: 270–285.

[19] Padmanabhan R, Oliveria MC, Alves JL, Menezes LF. Influence of process parameters on the deep drawing of stainless steel. *Finite Elements in Anal Des* 2007; 43:1062-1067.

[20] Reddy A, Rajesham S, Reddy PR, Kumar TP, Goverdhan J. An experimental study on effect of process parameters in deep drawing using Taguchi technique. *Int J Eng Sci Technol* 2015; 7(1):21-32.

[21] Atrian A, Fereshteh-Saniee F. Deep drawing process of Steel/brass laminated sheets. *Compos Part B* 2013; 47:75-81.

[22] Honarpisheh M, Niksokhan J, & Nazari F. Investigation of the effects of cold rolling on the mechanical properties of explosively-welded Al/St/Al multilayer sheet. *Metal Res Technol* 2016; 113(1): 105-113.

[23] Kasmaei M, Honarpisheh M. Investigation of annealing treatment on the mechanical and metallurgical properties of explosive-welded al/st/al multilayer. Journal: *Modares Mech Eng* 2015;15 (1): 397-402.

[24] Shojaeefard MH, Khalkhali A, Lahijani AT. Parametric Modal Study and Optimization of the Floor Pan of a B-Segment Automotive Using a Hybrid Method of Taguchi and a Newly Developed MCDM Model. *Latin Am J Solids Struct* 2016; 13: 3039-3061.

[25] Morovvati MR, Dariani BM, Asadidan MH. A theoretical, numerical, and experimental investigation of plastic wrinkling of circular two-layer sheet metal in deep drawing. *J Mater Proc Tech* 2010; 210:1738-1747.